Biodegradation (2011) 22:463–474
DOI 10.1007/s10532-010-9418-0

ORIGINAL PAPER

A kinetic analysis of three modified novel nitroreductases

Christopher D. Gwenin · Maher Kalaji · Peter A. Williams · Catherine M. Kay

Received: 30 June 2010 / Accepted: 14 September 2010 / Published online: 23 September 2010

Abstract A kinetic comparison between three nitroreductase enzymes isolated from the genome of *Bacillus licheniformis* ATCC 14580 for prospective use as immobilised enzymes for explosives detection has been conducted. The genes encoding the three enzymes (*yfkO* [BLNfnB] encoding an NfsB-like enzyme; *nfrA* [BLNfrA1] and *ycnD* [BLNfrA2] encoding PnrA-like enzymes) have been PCR amplified from the native genome and cloned into pET-28a(+) and a modified cysteine$_{(6)}$-tagged pET-28a(+) and subsequently over-expressed, purified, and biochemically characterised. The previously uncharacterised nitroreductases exhibited activity against a wide range of explosives, including cyclic nitramines. Amino acid alignments and overall structural comparisons with other nitroreductase family members suggest that the *B. licheniformis* enzymes are members of the NfsA-Frp/NfsB-FRase I family group. Despite the overall low amino acid identity, regions for flavin mononucleotide binding and active site residues were highly conserved.

Keywords *Bacillus licheniformis* · Nitroreductase · Explosives

C. D. Gwenin (✉) · M. Kalaji · P. A. Williams · C. M. Kay
School of Chemistry, Bangor University, Gwynedd LL57 2UW, United Kingdom
e-mail: c.d.gwenin@bangor.ac.uk

Introduction

Nitroreductase (NTR) are a family of proteins involved in the reduction of nitro-containing compounds utilising flavin mononucleotide (FMN) as cofactor. They are often homodimers and include the oxygen-insensitive NAD(P)H NTR NfnB (FMN-dependent NTR) (EC:1.5.1.34).

The NTR family of enzymes may be divided into two separate groups; flavin reductases such as FRase I from *Vibrio fischeri* (Zenno et al. 1994) and the classical NTRs from enteric bacteria (Watanabe et al. 1990; Bryant and DeLuca 1991; Bryant et al. 1991; Zenno et al. 1996a, b). Despite differences in flavin reductase activity both groups exhibit significant amino acid sequence homology and share very similar characteristics such as the ability to form a homodimer, a tightly associated FMN cofactor and a broad electron acceptor specificity.

NTR enzymes have been previously utilised in a number of applications including prodrug activation (Berne et al. 2006) for cancer treatment and in the detection of explosive compounds (Gwenin et al. 2008). In order to utilise a range of different substrate preferences/specificity to aid the identification of the explosive compounds, a number of NTRs have been genetically modified.

The NTR group can be further sub-divided into two groups: (1) oxygen-insensitive (type I), catalyzing a two-electron transfer from the reduced isoalloxazine ring of FMN to the nitro-substituted substrate with

the formation of nitroso or hydroxylamino derivatives, and (2) oxygen-sensitive (type II) NTRs which execute a one-electron transfer creating a 'futile cycle' where no net reduction of the nitro-containing compound occurs; instead a nitro-anion free radical is produced that rapidly reacts with oxygen to form superoxide, regenerating the parent nitro-compound in the process (Peterson et al. 1979). Oxygen-insensitive NTRs are further sub-divided into major and minor protein groups, examples being the *Escherichia coli* NfsA and NfsB enzymes, respectively. The major group has a specific requirement for NADPH as the electron donor whilst the minor group utilize either NADH or NADPH (Bryant et al. 1981; Whiteway et al. 1998).

The ability of bacterial enzymes to reduce nitro-aromatic compounds is widespread and NTR enzymes catalysing the reduction of explosive compounds such as 2,4,6-trinitrotoluene (TNT), hexahydro-1,3,5-trinitro-1,3,5-triazine (RDX) and nitroglycerine (NG) have been identified (Caballero et al. 2005; Lee et al. 2008; Gonzalez-Perez et al. 2007; Seth-Smith et al. 2002; Blehert et al. 1999). Reduction of TNT by *Pseudomonas* sp. strain JLR11 is catalyzed by PnrA and proceeds via a two-electron ping-pong Bi–Bi transfer mechanism to produce a hydroxylamino derivative with a stoichiometry of 2 mols of NADPH oxidised per mol of TNT and has a K_m value of 5 μM (Caballero et al. 2005). A second NTR form from JLR11 PnrB, showed negligible activity towards TNT in comparison with the PnrA. Lee et al. (2008) isolated and characterised a PnrB homologue (93% identity) from *Pseudomonas* sp. strain HK-6, a strain able to utilise TNT and RDX as sole nitrogen sources. Analysis of the kinetic parameters revealed high K_m (2.9 mM) and a V_{max} of 12.6 μmol min^{-1} mg^{-1}. A *pnrB*$^-$ knock-out strain demonstrated PnrB plays a major role in TNT degradation in vivo.

The NfsB from *E. coli* K12 exhibits a broad range of electron acceptor specificity including flavins, nitro compounds, quinones, and ferricyanides (Zenno et al. 1996a). It has also been shown to utilise a wide range of explosive compounds as electron acceptors; not only traditional explosive nitroaromatic compounds (i.e. TNT, 2,4,6-trinitrophenyl-*N*-methylnitramine (Tetryl), and picric acid) but also cyclic nitramine explosive compounds (Gwenin et al. 2008). Catalysis has been demonstrated to follow the ping-pong Bi-Bi mechanism with a 1:1 stoichiometry of the NAD(P)H oxidation reaction. The crystal structure, elucidated by Parkinson and co-workers (2000) shows that NfsB is a tightly associated homodimer with each subunit FMN bound within a crevice formed by the dimer interface. Increasing awareness of the threat of terrorist activity to national and global security has led to an urgent need to provide a rapid screening system for the detection of explosive compounds. In response an amperometric "nanodog" biosensor has been developed that exploits the properties of an immobilised *E. coli* K12 NfsB NTR, to facilitate explosive vapour detection in the part per trillion range (ppt) (Gwenin et al. 2007, 2008). The ability of the sensor to differentiate between different explosive compounds by using an array of enzymes each with a discernible signature response is under development.

To this end, three putative NTR enzymes have been isolated from the genome of the industrially important Gram-positive, soil bacterium *Bacillus licheniformis* ATCC 14580. The whole genome sequence of this bacterium is known, facilitating access to biotechnologically useful enzymes (Rey et al. 2004). The genes encoding the three enzymes (*yfkO* [BLNfnB] encoding an NfsB-like enzyme; *nfrA* [BLNfrA1] and *ycnD* [BLNfrA2] encoding PnrA-like enzymes) have been amplified by PCR from the native genome and cloned into pET-28a(+) and a modified cysteine$_{(6)}$-tagged pET-28a(+), pET-28a(+)cys$_6$ that has 6 cysteine codons inserted into the vector structure upstream of its multi-cloning site and downstream of the histidine tags. This vector has been constructed to facilitate enzyme immobilisation to form the biosensor (Gwenin et al. 2007). The three enzymes were over-expressed from *E. coli* Rosetta (pLysS DE3λ) with and without cysteine tags, purified, and characterised.

Materials and methods

Materials

Restriction enzymes and molecular biology products were obtained from Promega UK Ltd. The plasmid vector pET-28a(+) was purchased from Novagen. Explosive compounds were purchased as HPLC standards from Accustandard®, New Haven, USA. PCR reagents were purchased from BIOLINE UK and Qiagen. PCR primers, sequencing and oligonucleotides were purchased from Eurofins MWG Operon.

Plasmid and genomic DNA isolation kits were purchased from Qiagen and used according to manufacturer's instructions. Hi-trap affinity purification columns were purchased from GE Healthcare. Other chemicals were purchased from either Sigma-Aldrich or VWR International.

Blast searches

Homologues of *E. coli* K12 *nfnB*, *P. putida* JLR11 *pnrA,* and *B. subtilis* subsp. *subtilis* strain 168 *ycnD* were identified from either blastp and/or Conserved Domain Architecture Retrieval Tool (CDART) searches of the Genbank database. Amino acid alignments were performed using ClustalW2 (Gonnet protein matrix) (Larkin et al. 2007).

Bacterial strains and plasmids

Bacterial strains used and plasmids vectors used or constructed are listed in Table 1.

Cysteine-tag vector construction: pET-28a(+) modification

The protein expression vector pET28-a(+) (Novagen) was modified to contain six consecutive cysteine ($cys_{(6)}$) amino acid residues to function as an immobilisation tag replacing the pET-28(+) thrombin cleavage site at base pairs 127–144 of the pET-28a(+) expression/cloning region downstream of the N-terminal histidine-6 tag (base pairs 100–117). Two complementary oligonucleotides were synthesized. In addition to the cysteine-tag insertion a single base change was incorporated to remove the pET-28a(+) *Nhe*I site to aid in the identification of the new vector constructs. Forward oligonucleotide P28cF—5′-GGA GATATA*CCATGG*GCAGCAGC**CATCATCATCA TCATCAC**AGCAGCGGC***TGTTGCTGTTGCTGT TGC***CATATG***GGTAGC***ATGACTGGTGGACAGC AAATGGGTCGC*GGATCC*GAATTCG-3′ and reverse oligonucleotide p28cR—5′-CGAATTC*GGATCC*GC GACCCATTTGCTGTCCACCAGTCAT***GGTAGC***C ATATG***GCAACAGCAACAGCAACA***GCGCGTGC T**GTGATGATGATGATGATG**GCTGCTGC*CCAT GG*TATATCTCC-3′. (*Nco*I, *Bam*HI and *Nhe*I sites are shown underlined and in italics; the base-pair deleted to remove the *Nhe*I site is shown in bold type, His-tag residues are shown in bold type and underlined, the Cys-tag residues are shown in bold type, italicised and underlined). The complementary oligos were annealed together under the following conditions: 9 µl of each oligo and 2 µl of Proofstart™ PCR buffer were heat treated at 95°C for 30 s, 90°C for 30 s, 80°C for 30 s, 78°C for 120 s, 74°C for 60 s, 70°C for 30 s retained at

Table 1 Bacterial strains and plasmids used

	Description	Reference
Bacterial strains		
Bacillus licheniformis	Wild type	ATCC 14580
Escherichia coli DH5α	F^- ϕ80*lacZ*ΔM15 Δ(*lacZYA-argF*) U169 *deo*R *rec*A1 *end*A1 *hsd*R17 (r_K^-, m_K^+) *pho*A *sup*E44 *thi*-1 *gyr*A96 *rel*A1 λ^-	Promega
Escherichia coli strain Rosetta (DE3λ) pLysS	F^- *ompT hsdS*$_B$ (r_B^-, m_B^-) *gal dcm* (DE3λ) pLysSRARE (Cam^R)	Novagen
Plasmids used/constructed		
pET-28a(+)	Expression plasmid	Novagen
pET-28a(+)cys6	pET-28a(+) modified to include a $cys_{(6)}$-tag upstream of the multi-cloning site and downstream of the native His_6-sequence	This study
pBLNfnB	*B. licheniformis nfnB* (*yfkO*) cloned into pET-28a(+)	This study
pBLNfnB-Cys	*B. licheniformis nfnB* (*yfkO*) cloned into pET-28a(+)cys6	This study
pBLNfnBp1-Cys	*B. licheniformis nfnB* (*yfkO*) cys-tags incorporated into primer design	This study
pBLNfrA1	*B. licheniformis nfrA*1 (*nfrA*) cloned into pET-28a(+)	This study
pBLNfrA1-Cys	*B. licheniformis nfrA*1 (*nfrA*) cloned into pET-28a(+)cys6	This study
pBLNfrA2	*B. licheniformis nfrA*2 (*ycnD*) cloned into pET-28a(+)	This study
pBLNfrA2-Cys	*B. licheniformis nfrA*2 (*ycnD*) cloned into pET-28a(+)cys6	This study

4°C for 240 s. Annealed oligos were visualized by agarose gel electrophoresis (2% w/v). The annealed oligos and pET-28a(+) were digested with *Nco*I and *Bam*HI and ligated together. Self-ligated pET-28a(+) species were removed by *Nhe*I digestion and the pET-28a(+)cys6 construct was transformed into DH5α, transformants were selected for by *Nhe*I digestion inability. The construct was sequenced to verify the correct cys-tag insertion and used as an expression vector.

PCR primers

PCR primers are listed in Table 2. Oligonucleotide primers were designed using Lasergene software package (DNAstar, Inc., Madison, WI). Genes were amplified by PCR using Accuzyme DNA Polymerase (BIOLINE) according to manufacturer's instructions. PCR cycling conditions were: initial denaturation 95°C 5 min, 15 cycles of 94°C 1 min, 68–58°C 1 min, 72°C 1 min, followed by 25 cycles of 94°C 1 min, 58°C 1 min, 72°C 1 min with a final extension of 72°C for 10 min.

Gene cloning, expression, and purification

Molecular biology procedures were carried out according to standard protocols (Sambrook et al. 1989). Constructed plasmids were transformed into *E. coli* Rosetta pLysS (DE3λ) host cells for protein over-expression and purified as described previously (Gwenin et al. 2007). Purifications were visualised by sodium dodecyl sulphate-polyacrylamide gel electrophoresis (SDS-PAGE) 12 % w/v gels in a Lamelli buffer system using a BIO-RAD Protean 3 electrophoresis apparatus. Proteins were desalted using PD-10 desalting columns (GE Healthcare) and eluted with potassium phosphate buffer (PB) pH 7.0, 0.1 M. Protein concentrations were determined using Total protein reagent, Biuret method (Sigma) and BSA standards.

Enzyme kinetics

Enzyme kinetics were determined as NAD(P)H oxidation (μmol min^{-1}) from initial velocities taken over the first 15 or 30 s using an UVikon Kontron 943 spectrophotometer. Dinitroethylbenzene (DNEB) was used as

Table 2 PCR primers

Primer designation	Construct	Primer sequence 5′–3′	Restriction enzyme site	Bases changed to create restriction site italicised and underlined
BLnfnBBamF (forward primer)	pBLNfnB	GGAGA***GGATCC***AATATGACAGAGCAATCC	*Bam*HI	G*A*A*CAT* to form G*GATCC*
BLnfnBHindR (reverse primer)	pBLNfnB	ACCGCA***AAGCTT***TTATTCGACCCATTTCAC	*Hind*III	*GAAAAG* to form *AAGCTT*
BLnfrA1BamF (forward primer)	pBLNfrA1	AGGA***GGATCC***AGGATGAATAAAACGATTGAAA	*Bam*HI	GG*TAAG* to form GG*ATCC*
BLnfrA1SalIR (reverse primer)	pBLNfrA1	GGGGA***GTCGAC***TTACCTTTTGTTCAAA	*Sal*I	G*GTTC*C to formG*TCGA*C
BLnfrA2BamF (forward primer)	pBLNfrA2	AGGAT***GGATCC***CTAATGAATGAAGTATTGA	*Bam*HI	G*AGTTT* to form G*GATCC*
BLnfrA2HindR (reverse primer)	pBLNfra2	AGCCTA***AAGCTT***CTATTCGAGTTTAAATCC	*Hind*III	AAGC*A*T to form AAGC*TT*
BLnfnBBamFcys1 (forward primer) (reverse primer was BLnfnBHindR as described above)	pBLNfnBp1-Cys	GGAGA***GGATCC*****TGTTGCTGTTGCTGTTGC** AATATGACAGAGCAATCC[a]	*Bam*HI	G*A*A*CAT* to form G*GATCC*

The thermal cycling conditions were carried out as described in the "Materials and methods"

[a] Bases emphasized in bold indicate the $cys_{(6)}$-tag upstream of the gene sequence

the substrate with PB 0.1 M (pH 7.0) and 100 μM NAD(P)H as the external electron donor unless otherwise stated. The molar extinction co-efficient for NAD(P)H was taken as 6,220 M^{-1} cm^{-1}. For each assay, both blank and assay cuvettes contained NAD(P)H and enzyme solution to negate the effects of background NAD(P)H oxidation. Reactions were started by the addition of substrate to the assay cuvette.

[E] versus rate

The reaction rate was shown to increase proportionally with enzyme concentration. An enzyme concentration, within the linear portion of the measured enzyme dependent rate, was used in further experiments.

[S] versus rate

Substrate-dependent rates were determined using constant enzyme and NAD(P)H concentrations with a range of different substrate concentrations. The kinetic parameters, K_m and V_{max} were calculated from initial velocities and analysed by direct linear analysis using EnzPack programme (Williams and Zaba 1997), which calculates the most probable values for the kinetic parameters with their 68% confidence limits. Each velocity was determined in triplicate using separate enzyme purifications.

pH optimum

The pH optimum was determined as μmoles of NAD(P)H oxidised min^{-1} at 340 nm using 0.1 M of the following buffers: PB (pH 3.0–10.0), glycine-NaOH (pH 8.0–11.0), citrate (pH 3.0–6.0) and Tris-HCl (pH 5.0–11.0).

Thermal stability

Enzyme thermal stability was determined by incubating aliquots of enzyme preparations for 15 min at varying temperatures (0–70°C). Analysis of residual enzyme activity was assayed after a 15 min recovery time at room temperature.

Substrate specificity

Enzyme substrate specificities were determined as specific activity (μmol min^{-1} mg^{-1}) by monitoring NAD(P)H oxidation using 10 μM of each substrate to enable direct comparison of the reaction rates. For accurate determination of enzyme activity with each substrate an equal amount of the substrate solvent was added to the blank cuvette to negate any solvent effects on NAD(P)H oxidation.

Stoichiometry

Using an excess of [NAD(P)H] over [substrate] the stoichiometry was calculated by determining the total diminution of [NAD(P)H] associated with completion of the reaction. The substrate used was DNEB and stoichiometric measurements were made using substrate concentrations between 10 and 100 μM.

Genbank accession numbers

Bacillus licheniformis NfnB (YfkO)—YP_078038, *B. licheniformis* NfrA1—YP_081098, *B. licheniformis* NfrA2—YP_077707.

Results

Blast searches

The *B. licheniformis* NfrA homologues were identified from blastx and blastp searches of the Genbank database (Table 3) using the *P. putida* JLR11 PnrA (NfsA-Frp type) as a search probe. The *B. licheniformis* NfrA homologues were therefore presumed to belong to the NfsA-Frp family of oxidoreductase NADPH-dependent nitro/flavin reductases. The *B. licheniformis* NfnB homologue was identified from secondary searches using protein homologues identified using the *E. coli* K12 NfnB (NfsB-Frp type) as a probe for blastx, blastp and Conserved Domain Architecture Retrieval Tool (CDART) searches of the Genbank database (Table 3).

Cloning and expression

The pET-28a(+) cloned genes were sub-cloned into pET-28a(+)cys6 providing a $His_{(6)}$-tagged and $Cys_{(6)}$-tagged protein sequence for (1) purification (His) and (2) protein immobilisation (Cys). The constructs were transformed into *E. coli* Rosetta pLysS (DE3λ) host cells for protein over-expression.

Table 3 *Bacillus licheniformis* NfnB and PnrA homologues cloned and expressed

Homologous protein	Putative gene laboratory designation protein product	Gene size amino acid residues MW	Amino acid % identity/% similarity to *E. coli* K12 NfnB and *P. putida* JLR11 PnrA
E. coli K12 NfnB	*yfkO*	685 bp	25/45
	BLnfnB	227 residues	
	NfsB-like NTR NAD(P)H:FMN oxidoreductase family	26 kDa	
P. putida JLR11 PnrA	*nfrA*	750 bp	33/59
	BLNfrA1	249 residues	
	NADPH-linked nitro/flavin reductase NfsA-like	28 kDa	
P. putida JLR11 PnrA	*ycnD*	738 bp	36/54
	BLNfrA2	245 residues	
	NAD(P)H-linked nitro/flavin reductase NfsA-like	27 kDa	

A bright yellow colour in the cell-free extract, on the column and as the final purification elution mixture indicated the presence of a flavoprotein. Enzyme purification was achieved for all enzymes cloned into the unmodified pET-28a(+) (Fig. 1a–c).

The constructs BLNfrA1-Cys and BLNfrA2-Cys expressed from the pET-28a(+)cys6 vector were both column purified (Fig. 1e, f).

In the case of BLNfnB-Cys, over-expressed protein was observed in crude lysis experiments and in the cell free extract but did not bind to the purification column, this could be due to an alternate quaternary structure of the protein causing the His-tags to be located internally and not at the protein surface.

To obtain purified BLNfnB-Cys, the six cysteine codons were incorporated into the structure of the forward primer, BLNfnBBamFcys1 (Table 2), moving the cysteine tags 45 bases closer to the gene's ATG translational start site so that they were separated from the N-terminus of the protein by only one amino acid residue. Re-cloning this DNA fragment into pET-28a(+), created pBLNfnBp1-Cys (Table 1) and resulted in an over-expressed protein product that bound to the column and was purified (approximately 95% pure protein) (Fig. 1d).

Enzyme kinetics

Enzyme concentration versus reaction rate

The rate of the BLNfnBp1-Cys, BLNfrA1-Cys, and BLNfra2-Cys enzyme reactions were measured as initial reaction rates. The rate of NAD(P)H oxidation was shown to be proportional to the amount of enzyme present in the assay. All measured initial rates were within a 5% error margin.

Substrate concentration versus reaction rate

The kinetic parameters K_m and V_{max} were determined in 0.1 M PB (pH 7) for purified BLNfra1-Cys, BLNfrA2-Cys, BLNfnBp1-Cys, and the non-cysteine tagged enzymes by varying the substrate concentration, in the presence of a constant concentration of 100 μM NAD(P)H. Hyperbolic curves were produced, indicative of Michaelis-Menten kinetics and were analysed as stated in "Materials and methods". A comparison of K_m and V_{max} values generated can be seen in Table 4. Apparent differences in K_m and V_{max} between the BLNfnB and BLNfrA1 tagged and non-tagged enzymes indicate the incorporated cysteine residues affect the catalytic reaction: For BLNfnBp1-Cys a marginal increase in K_m and a decrease in the V_{max} value are seen compared to BLNfnB, indicating an overall negative effect on the turnover and the affinity. However, in the case of BLNfrA1-Cys, the observed effect of lowered K_m and decreased V_{max} indicates that the enzyme-substrate binding is enhanced (K_m is reduced),but the enzyme-substrate complex reacts more slowly (V_{max} is reduced). No such effects were observed with BLNfrA2-Cys. This enzyme had a much greater affinity for the DNEB substrate than the BLNfnB and BLNfrA1 enzymes but a low reaction velocity (K_m 26 μM and V_{max}

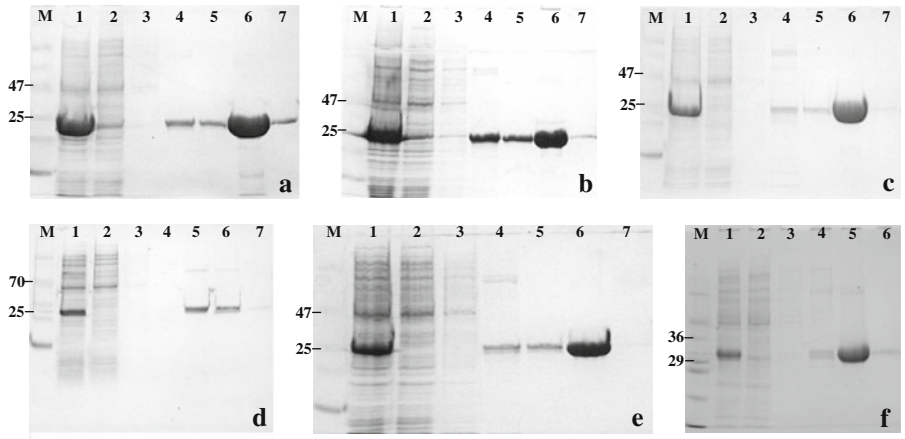

Fig. 1 **a** BLNfnB protein purification. SDS-PAGE. *M* Protomarker™ molecular marker. *Lane 1* cell free extract, *Lane 2* Sample flow through, *Lane 3* Wash flow through 20 mM imidazole, *Lane 4* 100 mM imidazole fraction-2, *Lane 5* 100 mM imidazole fraction-5, *Lane 6* 500 mM imidazole (*bright yellow* fraction-2), *Lane 7* 500 mM fraction-5. **b** BLNfnA1 protein purification. SDS-PAGE. *M* Protomarker™ molecular marker. *Lane 1* Cell free extract, *Lane 2* Sample flow through, *Lane 3* Wash flow through 20 mM imidazole, *Lane 4* 100 mM imidazole fraction-2, *Lane 5* 100 mM imidazole fraction-5, *Lane 6* 500 mM imidazole fraction-2 (*bright yellow* fraction), *Lane 7* 500 mM imidazole fraction-5. **c** BLNfrA2 protein purification. SDS-PAGE. *M*. Protomarker™ molecular marker. *Lane 1* Cell free extract, *Lane 2* Sample flow through, *Lane 3* Wash flow through 20 mM imidazole, *Lane 4* 100 mM imidazole fraction-2, *Lane 5* 100 mM imidazole fraction-5, *Lane 6* 500 mM imidazole fraction-2, *Lane 7* 500 mM imidazole fraction-5. **d** BLNfnBp1-Cys protein purification SDS-PAGE. *M* Protomarker™ molecular marker. *Lane 1* Cell free extract, *Lane 2* Sample flow through, *Lane 3* Wash flow through 20 mM imidazole, *Lane 4* 100 mM imidazole fraction-2, *Lane 5* 500 imidazole fraction-2 (*bright yellow*), protein size 26 kDa, *Lane 6* 500 mM imidazole fraction-3 (*bright yellow*), *Lane 7* 500 mM imidazole fraction-5. **e** BLNfrA1-Cys purification. SDS-PAGE. *M* Protomarker™ molecular marker. *Lane 1* Cell free extract, *Lane 2* Sample flow through, *Lane 3* Wash flow through 20 mM imidazole, *Lane 4* 100 mM imidazole fraction-2, *Lane 5* 100 imidazole fraction-5, *Lane 6* 500 mM imidazole fraction-2 (*bright yellow*), protein size 29 kDa, *Lane 7* 500 mM imidazole fraction-5. **f** BLNfrA2-Cys purification. SDS-PAGE. *M* Sigma low weight molecular marker. *Lane 1* Cell free extract, *Lane 2* Sample flow through, *Lane 3* Wash flow through 20 mM imidazole, *Lane 4* 100 mM imidazole fraction-2, *Lane 5* 500 mMimidazole fraction-2 (*bright yellow*), protein size 27 kDa, *Lane 6* 500 mM imidazole fraction-2

5 μmol min^{-1} mg^{-1}). Overall when the experimental variation is considered there is no general trend induced with the incorporation of the cys tags.

pH optimum

The pH profiles of BLNfnBp1-Cys, BLNfrA1-Cys, and BLNfrA2-Cys were determined in a range of buffer solutions. BLNfnBp1-Cys (Fig. 2a) displayed a narrow optimal pH peak in PB of pH 7.0. BLNfrA1-Cys (Fig. 2b) showed a broad pH optimum between pH 5.0 and 9.0, which corresponded well with the other buffer solutions used. In comparison, BLNfrA2-Cys (Fig. 2c) exhibited a narrow pH optimum in PB of pH 5.0. The activity observed with 0.1 M glycine-NaOH, citrate, and tris-HCl buffers was much reduced in comparison, indicating that the enzyme activity was optimal only in PB.

Thermal stability

Both BLNfnBp1-Cys and BLNfrA2-Cys were thermally stable up to 50°C (Table 4). At 60°C BLNfnBp1-Cys retained 80% of activity after 15 min, whereas BLNfrA2-Cys retained 40% of enzyme activity (data not shown). BLNfrA1-Cys (Table 4) was thermally stable up to 60°C. Further temperature increments caused rapid protein denaturation and loss of enzyme activity. Therefore all three enzymes show high thermal tolerance with BLNfnrA1-Cys the more heat stable up to 60°C.

Substrate specificity

The preference of the enzymes for different explosive compounds was determined by comparing the NAD(P)H oxidation rates at an identical concentration of each of the substrates (Fig. 3). The concentration

Table 4 Direct linear kinetic data analyses performed by (68% confidence limits), maximum thermal stability and stoichiometric profile

Enzyme	K_m (μM) (range)	V_{max} (μmol min^{-1} mg^{-1}) (range)	V_{max}/K_m	Maximum thermal stability[a]	Stoichiometric ratio NAD(P)H:DNEB[b]
BLNfnBp1-Cys	540 (344–771)	10 (8.87–11.1)	0.02	50	1.02:1.00
BLNfnB	450 (307–507)	33 (30.0–35.9)	0.07	ND	ND
BLNfrA1-Cys	330 (290–356)	16 (14.3–16.1)	0.05	60	2.14:1.00
BLNfrA1	490 (272–696)	35 (32.2–43.4)	0.07	ND	ND
BLNfrA2-Cys	26 (21.1–40.8)	5 (4.26–5.64)	0.19	50	0.99:1.00
BLNfrA2	27 (19.3–31.4)	5 (4.81–5.83)	0.20	ND	ND

[a] Maximum thermal stability taken as 100% of NAD(P)H oxidation activity retained after heat treatments of the enzymes (0–70 °C) for 15 min

[b] Micromole of NAD(P)H consumed:micromole of DNEB present

ND not done

of the substrates was kept identical to avoid any alteration in rate comparisons due to changes in Michaelis constant values.

A distinctive pattern can be observed in the enzymatic response to the different nitroaromatic and explosives tested (Fig. 3). Most obvious is the high activity of BLNfrA1-Cys against the explosive compounds TNT and Tetryl (specific activities 30 and 35 μmol min^{-1} mg^{-1}, respectively), approximately 10- and 7-fold higher than the responses of BLNfnBp1-Cys and BLNfrA2-Cys.

For picric acid, a structure that also carries nitro groups at the 2,4,6 positions of the aromatic ring, all three enzymes showed a similar activity. An especially marked decrease in specific activity against picric acid was observed for BLNfrA1-Cys in comparison with that observed against TNT and Tetryl. This may be due to the reactive nature of the phenol group of picric acid affecting the entry or binding of this compound to the active site of the enzyme. BLNfrA1-Cys exhibits a diverse response to the compounds used and is active with the explosive compounds TNT, Tetryl, picric acid, ethylene glycol dinitrate (EGDN). Compounds that are not substrates for BLNfrA1-Cys are 1,3-dinitrato-2,2-bis(nitratomethyl)propane (PETN), RDX, NG, and octahydro-1,3,5,7-tetranitro-1,3,5,7-tetrazocine (HMX) (Fig. 3)

BLNfnBp1-Cys showed no activity with RDX and HMX whereas BLNfrA2-Cys showed low but measurable levels of activity with the entire range of explosive compounds.

BLNfrA1-Cys, BLNfnBp1-Cys, and BLNfrA2-Cys exhibited a clear preference for TNT and Tetryl as substrates. All three enzymes produced a defined signature response to the explosive and nitro-aromatic compounds tested, hence providing much promise at distinguishing the explosive compounds present.

Stoichiometry

The stoichiometry of micromole of NAD(P)H oxidation per micromole of substrate molecule was determined for BLnfnBp1-Cys, BLNfrA1-Cys, and BLNfrA2-Cys (Table 4). UV-analysis monitoring of NAD(P)H concentration showed a stoichiometric decrease in NAD(P)H that corresponded to a ratio of 1:1 for BLNfnBp1-Cys, 2:1 for BLNfrA1-Cys, and 1:1 for BLNfrA2-Cys. A strong NAD(P)H oxidase activity in the absence of substrate was observed for

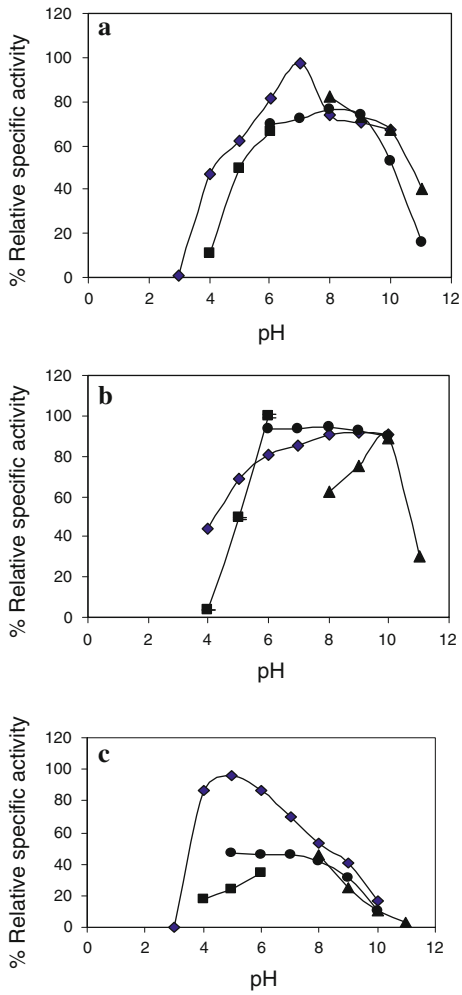

Fig. 2 pH profiles were determined using potassium phosphate, citrate, glycine–NaOH and tris–HCl buffers at 0.1 M concentrations. The relative specific activity is expressed as the percentage of the maximum specific activity attained under the experimental conditions. **a** BLNfnBp1-Cys. **b** BLNfrA1-Cys. **c** BLNfrA2-Cys. *Diamond* potassium phosphate, *square* citrate, *triangle* glycine–NaOH. *circle* tris–HCl. Standard deviations were below ± 10%

all three enzymes, however because this activity was blanked out be the reference cuvette this does not impede the overall sensor design.

Discussion

Three *B. licheniformis* flavoprotein enzymes, BLNfnB, BLNfrA1 and BLNfrA2 belonging to the NfsA-Frp and NfsB/FRase I NTR family have been cloned with the addition of a $cys_{(6)}$- tag in *E. coli*, over-expressed, purified and characterized. The non-cysteine tagged enzymes BLNfnB and BLNfrA1 displayed similar kinetic parameters (K_m and V_{max}) for the DNEB substrate (Table 4). Incorporation of the cysteine residues into their protein structures affected the catalytic activities, although no overall general trend was induced. The kinetic parameters for BLNfrA2 were unaffected by the cysteine tag addition.

The three cysteine tagged enzymes displayed marked differences in pH profiles BLNfnBp1-Cys and BLNfrA2-Cys showed a narrow peaks of activity at pH 7.0 and pH 5.0 in 0.1 M PB (Fig. 2a, c), whilst BLNfrA1-Cys displayed a broad pH range, with maximal activity occurring between pH 6.0 and pH 9.0 (Fig. 2b). BLNfnBp1-Cys and BLNfrA2-Cys were active with NADH, whereas BLNfrA1-Cys had an absolute requirement for NADPH, BLNfnBp1-Cys and BLNfrA2-Cys were both thermally stable up to 50°C and both had a NADH oxidation stoichiometry of 1:1 with DNEB (Table 4). BLNfrA1-Cys was thermally stable up to 60°C and displayed a NADPH oxidation stoichiometry of 2:1 with DNEB (Table 4). The BLNfnBp1-Cys enzyme was expressed in a slightly lower yield indicating that the protein may be being expressed as inclusion bodies due to a change in structure cursed by the insertion of the Cys tags. This assumption is supported by the impact on the V_{max}. Future work will focus on altering the position of the Cys tags.

Amino acid alignments BLNfrA1 and BLNfrA2

The BLNfrA1 and BLNfrA2 amino acid sequences were aligned with those of the *E. coli* NfsA and the JLR11 PnrA (Fig. 4). The aligned proteins shared similar levels of identity and similarity (between 32–41% identity and 49–61% similarity). Nitroreductase enzymes have conserved domains required for interaction with cofactor, electron donor and nitroaromatic substrates. Conserved domains for FMN binding have been identified in BLNfrA1 and BLNfrA2 by amino acid alignment (Fig. 4). Comparisons of NADPH binding residues and those residues forming the active site cleft in NfsA (Kobori et al. 2001) and JLR11 PnrA (Caballero et al. 2005) are also well conserved in BLNfrA proteins although BLNfrA2 shows more variation in NADPH binding residues.

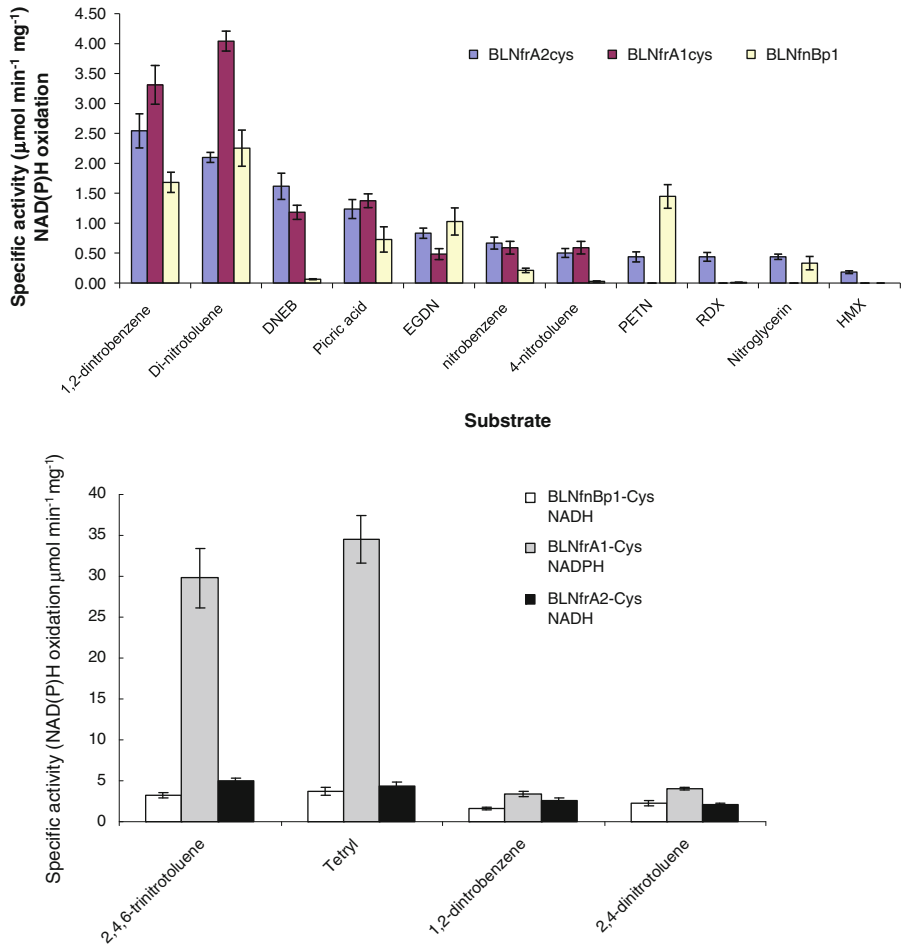

Fig. 3 BLNfnBp1-Cys, BLNfrA1-Cys and BLNfrA2-Cys substrate specificity. Substrate specificity measurements (Specific activity µmol min^{-1} mg^{-1}) were performed using 100 µM NADH, 10 µM of each substrate, and an equal volume of the appropriate substrate solvents in the blank cuvette to minimise background NADH oxidation. Two separate graphs are shown to give better clarity at the lower levels of specific activity. *Error bars* are representative of the standard deviation ($\pm n = 3$)

Amino acid alignment BLNfnB

BLNfnB was aligned with members of the NTR family, *E. coli* K12 NfnB, the *Enterobacter cloacae* NTR and *V. fischeri* FRase I (Fig. 5). BLNfnB shared low % identity/% similarity homologies with the other aligned enzymes (20%/42%). The *E. coli* NfnB and the *E. cloacae* NTR are highly similar (88%/92%) but have 32%/50% identity/similarity with FRase I. From the amino acid alignment, regions of amino acid conservation that correspond to FMN binding regions are observed (Fig. 5). BLNfnB shows the greatest variation from the other NTR structures within the central and the C-terminal regions. This correlates to overall structural similarities of the ECNfnB monomer where the greatest variations between NfnB and FRaseI occur between residues 90–134 and 181–206 (Parkinson et al. 2000). The amino acid region 90–134 confers substrate specificity in the *E. coli* NfnB and contains Phe124 an important active site residue for reductase activity as substitution of this residue conferred flavin reductase activity to NfnB (Zenno et al. 1996c). This residue however does not appear to be conserved in the BLNfnB sequence. The amino acid alignments and overall structural comparisons with other NTR family members suggest that the

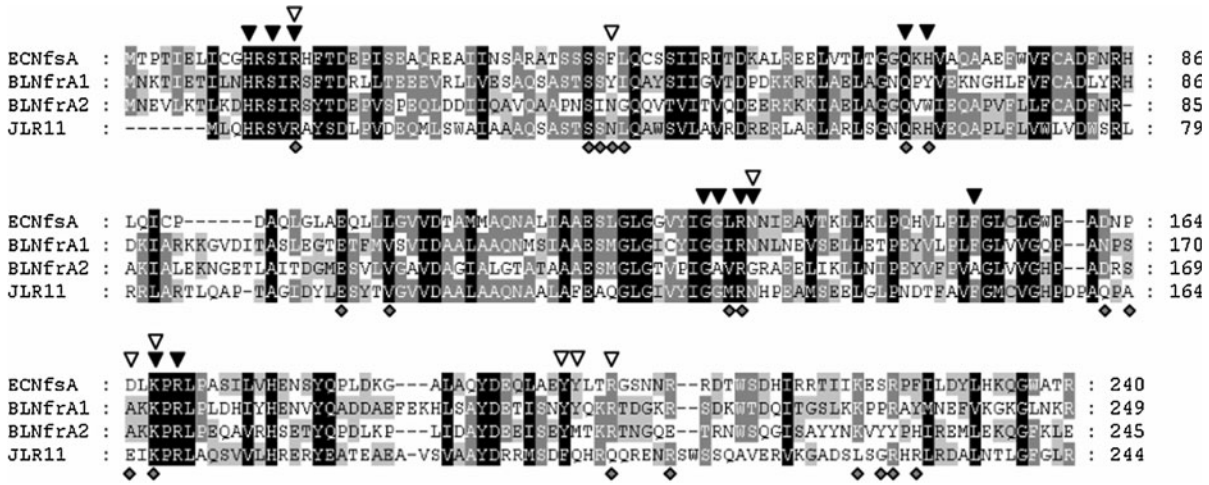

Fig. 4 Amino acid alignment of BLNfrA1 and BLNfrA2 with PnrA and NfsA. JLPnrA—*P. putida* JLR11 PnrA—accession number AAM95986. ECNfsA—*E. coli* K12 NfsA—accession number NP_415372. BLNfrA1—*B. licheniformis* NfrA1—accession number YP_081098. *B. licheniformis* NfrA2—accession number YP_077707. *Black triangles* indicate FMN binding sites, *white triangles* indicate NADPH binding sites, *grey diamonds* under sequences indicate residues whose side chains form the active site cleft in NfsA (data taken from NfsA crystal structure, Kobori et al. 2001)

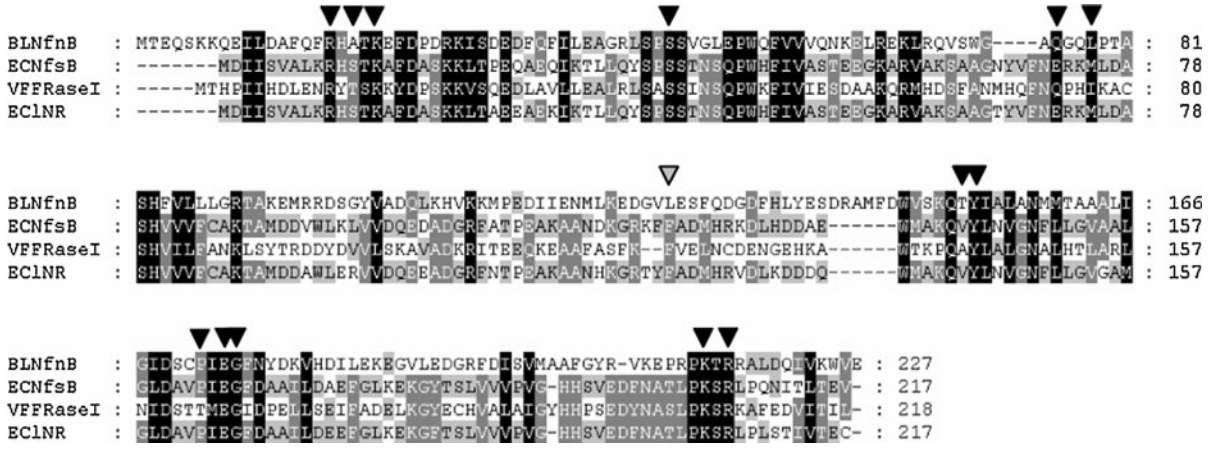

Fig. 5 Amino acid alignment of BLNfnB with the *E. coli* K12 NfnB, the *E. cloacae* NTR and *V. fischeri* FRase I. *E. coli* K12 NfnB accession number—BAA05004. *E. cloacae* NTR accession number—AAA62801. *V. fischeri* FRase I accession number—BAA04595. *Black triangles* indicate FMN binding regions (data derived from the K12 NfsB crystal structure (Parkinson et al. 2000). *Black triangles* indicate residues involved in FMN binding. The *grey triangle* indicates Phe124 an important residue for flavin/nitro reductase activity within the *E. coli* NfnB (Zenno et al. 1996c; Parkinson et al. 2000)

B. licheniformis enzymes are members of the NfsA-Frp/NfsB-FRase I family group (Figs. 4, 5). Despite the overall low amino acid identity, regions for FMN binding and active site residues were highly conserved.

In the substrate specificity investigations the three enzymes exhibited activity against a wide range of explosive compounds, including cyclic nitramines (Fig. 3). However, the resulting data also illustrates that when analyzing a sample containing an unknown concentration of an unknown compound, if you obtain a signal with BLNfrA2-Cys and no signal with both other enzymes, you will be unable to know if the compound in the analyzed sample is RDX or HMX. The same comment can be made concerning 1,2-dinitrobenzene and picric acid. Consequently in order to produce a commercial array sensor more enzymes of varying structures are required.

The optimum conditions of the enzymes and their required cofactor would not restrict the development of a sensor; we propose to utilize separate micro cuvettes for each individual type of nitroreductase.

Acknowledgment The authors wish to acknowledge funding from Trwyn and Nanosecure an EU project.

References

Berne C, Betancor L, Luckarift HR, Spain JC (2006) Application of a microfluidic reactor for screening cancer prodrug activation using silica-immobilized nitrobenzene nitroreductase. Biomacromolecules 7:2631–2636

Blehert DS, Fox BG, Chambliss GH (1999) Cloning and sequence analysis of two *Pseudomonas* flavoprotein xenobiotic reductases. J Bacteriol 181:6254–6263

Bryant C, DeLuca M (1991) Purification and characterization of an oxygen-insensitive NAD(P)H nitroreductase from *Enterobacter cloacae*. J Biol Chem 266:4119–4125

Bryant DW, McCalla DR, Leeksma M, Laneuville P (1981) Type I nitroreductases of *Escherichia coli*. Can J Microbiol 27:81–86

Bryant C, Hubbard L, McElroy WD (1991) Cloning, nucleotide sequence, and expression of the nitroreductase gene from *Enterobacter cloacae*. J Biol Chem 266:4126–4130

Caballero A, Lazaro JJ, Ramos JL, Esteve-Nunez A (2005) PnrA a new nitroreductase-family enzyme in the TNT-degrading strain *Pseudomonas putida* JLR11. Environ Microbiol 7(8):1211–1219

Gonzalez-Perez M, van Dillewijn MP, Wittich RM, Ramos JL (2007) *Escherichia coli* has multiple enzymes that attack TNT and release nitrogen for growth. Environ Microbiol 9:1535–1540

Gwenin CD, Kalaji M, Williams PA, Jones RM (2007) The orientationally controlled assembly of genetically modified enzymes in an amperometric biosensor. Biosens Bioelectron 22:2869–2875

Gwenin CD, Kalaji M, Kay CM, Williams PA, Tito DN (2008) An in situ amperometric biosensor for the detection of vapours from explosive compounds. Analyst 133:621–625

Kobori T, Sasaki H, Lee WC, Zenno S, Saigo K, Murphy MEP, Tanokura M (2001) Structure and site-directed mutagenesis of a flavoprotein from *Escherichia coli* that reduces nitrocompounds. Alteration of pyrimidine nucleotide binding by a single amino acid substitution. J Biol Chem 276:2816–2823

Larkin M, Blackshields AG, Brown NP, Chenna R, McGettigan PA, McWilliam H, Valentin F, Wallace IM, Wilm A, Lopez R, Thompson JD, Gibson TJ, Higgins DG (2007) Sequence analysis. Clustal W and Clustal X version 2.0. Bioinformatics 23:2947–2948

Lee B-U, Park S-C, Cho Y-S, Kahng H-Y, Oh K-H (2008) Expression and characterization of the TNT nitroreductase of *Pseudomonas* sp. HK-6 in *Escherichia coli*. Curr Microbiol 56:386–390

Parkinson GN, Skelly JV, Neidle S (2000) Crystal structure of FMN-dependent nitroreductase from *Escherichia coli* B: a prodrug activating enzyme. J Med Chem 43:3624–3631

Peterson FJ, Mason RP, Hovsepian J, Holtzman JL (1979) Oxygen-sensitive and -insensitive nitroreduction by *Escherichia coli* and rat hepatic microsomes. J Biol Chem 254:4009–4014

Rey MW, Ramaiya P, Nelson BA, Brody-Karpin SD, Zaretsky EJ, Tang M, de Leon AL, Xiang H, Gusti V, Clausen IG, Olsen PB, Rasmussen MD, Andersen JT, Jorgensen PL, Larsen TS, Sorokin A, Bolotin A, Lapidus A, Galleron N, Ehrlich SD, Berka RM (2004) Complete genome of the industrial bacterium *Bacillus licheniformis* and comparisons with closely related *Bacillus* species. Genome Biol 5:R77

Sambrook J, Fritsch EF, Maniatis T (1989) Molecular cloning: a laboratory manual, 2nd edn. Cold Spring Harbor Laboratory Press, New York

Seth-Smith HMB, Rosser SJ, Basran A, Travis ER, Dabs ER, Nicklin S, Bruce NC (2002) Cloning, sequencing and characterization of the hexahydro-1,3,5-trinitro-1,3,5-triazine degradation gene cluster from *Rhodococcus rhodochrous*. Appl Environ Microbiol 68:4764–4771

Watanabe M, Ishidate M Jr, Nohmi T (1990) Nucleotide sequence of *Salmonella typhimurimum* nitroreductase gene. Nucleic Acids Res 18:1059

Whiteway J, Koziarz P, Veall J, Sandhu N, Kumar P, Hoecher B, Lambert IB (1998) Oxygen-insensitive nitroreductases: analysis of the roles of *nfsA* and *nfsB* in development of resistance to 5-nitrofuran derivatives in *Escherichia coli*. J Bacteriol 180:5529–5539

Williams PA, Zaba BN (1997) EnzPack for Windows. Biosoft, Cambridge, UK

Zenno S, Saigo K, Kanoh H, Inouye S (1994) Identification of the gene encoding the major NAD(P)H-flavin oxidoreductase of the bioluminescent bacteria *Vibrio fischeri* ATCC 7744. J Bacteriol 176:3536–3543

Zenno S, Koike H, Tanokura M, Saigo K (1996a) Gene cloning, purification, and characterization of NfsB, a minor oxygen-insensitive nitroreductase from *Escherichia coli*, similar in biochemical properties to FRase I, the major flavin reductase in *Vibrio fischeri*. J Biochem 120:736–744

Zenno S, Koike H, Kumar AN, Jayaraman R, Tanokura M, Saigo K (1996b) Biochemical characterization of NfsA, the *Escherichia coli* major nitroreductase exhibiting a high amino acid sequence homology to Frp, a *Vibrio harveyi* flavin oxidoreductase. J Bacteriol 178:4508–4514

Zenno S, Koike H, Tanokura M, Saigo K (1996c) Conversion of NfsB, a minor *Escherichia coli* nitroreductase, to a flavin reductase similar in biochemical properties to FRase I, the major flavin reductase in *Vibrio fischeri*, by a single amino acid substitution. J Bacteriol 178:4731–4733